Title
CARBON PARTICULATE IN SMALL POOL FIRE FLAMES

Authors
Bard, S.
Pagni, P.J.

Publication Date
1981-05-01

LBL-12766
Preprint

Lawrence Berkeley Laboratory
UNIVERSITY OF CALIFORNIA

ENERGY & ENVIRONMENT DIVISION

To be published in the Journal of Heat Transfer, Transactions of American Society of Mechanical Engineers, Series C

CARBON PARTICULATE IN SMALL POOL FIRE FLAMES

S. Bard and P.J. Pagni

May 1981

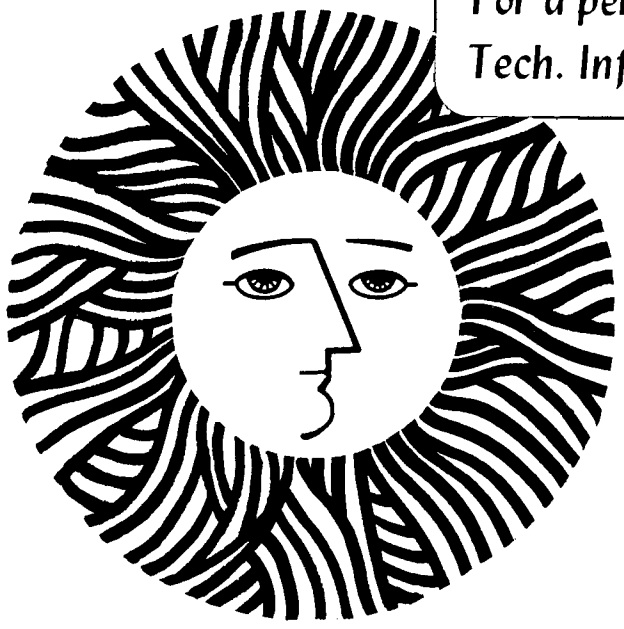

Prepared for the U.S. Department of Energy under Contract W-7405-ENG-48

DISCLAIMER

CARBON PARTICULATE IN SMALL POOL FIRE FLAMES

by

S. Bard[†] and P. J. Pagni
Mechanical Engineering Department and
Lawrence Berkeley Laboratory
University of California
Berkeley, CA. 94720

The authors are grateful for support from the Center for Fire Research of the National Bureau of Standards, under Grant No. NB 80 NAG-E6839 which was administered by the U.S. Department of Energy under Contract W-7405-ENG-48.

[†] current address: Thermal Science and Engineering Group
Jet Propulsion Laboratory
4800 Oak Grove Drive
Pasadena, CA 91103

This manuscript was printed from originals provided by the author.

Abstract

Flame radiation, the dominant heat transfer mechanism in many combustion and fire safety related problems, is primarily controlled by the fraction of flame volume occupied by solid carbon particulate. A multi-wavelength laser transmission technique is used here to measure carbon particulate volume fractions and approximate particle size distributions in ten common solid, cellular and liquid fueled small scale, O (10 cm dia), pool fire diffusion flames. The most probable particle radius, r_{max}, and concentration, N_o, are two parameters in the assumed gamma function size distribution form which are determined for each fuel by simultaneously measuring light transmission of two superimposed laser wavelengths. The resulting soot volume fractions range from $f_v \sim 4 \times 10^{-6}$ for cellular polystyrene to $f_v \sim 7 \times 10^{-8}$ for alcohol. Cellular polystyrene has the largest particles, $r_{max} \sim$ 60nm while wood has the smallest, $r_{max} \sim$ 20nm. The carbon particulate optical properties used in the analysis are shown to be representative of actual flame soot and are more accurate than the soot refractive index usually assumed in the literature. Finally, mean particle sizes obtained for all fuels indicate that the small particle absorption limit assumption is a reasonable approximation for infrared flame radiation calculations.

INTRODUCTION

Flame radiation, the dominant heat transfer mode in many combustion problems [1], is strongly influenced by the fraction of flame volume occupied by solid carbon particulate. Carbon particulate formation processes have been studied for many years but it is not yet possible to predict flame particle size distributions and concentrations. Thus, experimental methods for characterizing flame soot are necessary and important. A multi-wavelength laser transmission technique is reported here to determine "in situ" carbon particulate volume fractions and size distributions. Ten common solid, cellular, and liquid hydrocarbon fueled, small scale O (10 cm) buoyant diffusion flames are studied.

Optical techniques for characterizing particulates are attractive due to their non-intrusive nature. However, accurate soot refractive indices as a function of wavelength are required in any light scattering [2-8] transmission [9, 10] or radiance [11, 12] experiment from which particulate volume fractions and size distributions are to be deduced. There has existed some uncertainty regarding the soot refractive index, $m = n(1 - ik)$. Diffusion flame soot volume fractions and size distributions previously reported [3, 8, 10, 12] were based on the refractive indices reported by Dalzell and Sarofim [13] based on reflectance measurements from compressed soot samples, (e.g., $m = 1.57 - 0.56\,i$ at 488nm). However, the Ref. 13 values may be in error due to the presence of unavoidable voids in the compressed soot. Medalia and Richards [14] estimate from compressibility data that the compressed soot of Ref. 13 is actually 1/3 air by volume. Based on this void volume fraction, Graham [15] estimates that Dalzell and Sarofim's n and nk may be 20% low.

Also, Chippet and Gray [16] combined electronmicrographic particle size analysis and spectral transmission measurements to obtain an average m = 1.9-0.35i in the visible wavelength range. Absorption of incident radiation by gaseous molecules or radicals may have slightly affected the results obtained from their premixed acetylene flames [8, 17]. Recently, in situ soot optical properties, improved over Ref. 13 in the direction suggested above [14-16] , have been reported by Lee and Tien [18]. They propose a dispersion model based on a rigorous consideration of carbon particle electron band structure. Dispersion constants are determined from independent transmission measurements in polymethylmethacrylate and polystyrene fueled flames at visible [10] and infrared wavelengths [12]. Their soot optical properties, reflecting values of actual flame soot, are summarized in Table 1 for several wavelengths.

There is good agreement of the Table 1 optical properties with the Chippet and Gray [16] results and with the corrections to Ref. 13 indicated by Graham [15]. The soot refractive index was shown in Ref. [18] to be rather insensitive to fuel hydrogen/carbon ratio and to temperature, in the range of typical flame temperatures. The multiwavelength laser transmission techniqued developed here determines particulate volume fractions and size distributions from the ratios of experimentally measured extinction coefficients at several different wavelengths. This technique is used [18] to demonstrate that the Ref. 13 optical properties produce particle sizes and volume fractions which are not consistent at different wavelength combinations. In some cases the extinction coefficient ratios actually exceed the theoretical limit [18]. However, when Lee and Tien's optical properties (Table 1) are used, the resulting volume fractions and size distributions are consistent at every

extinction coefficient ratio. The previous arguments lead to the conclusion that the Table 1 soot optical properties are valid as mean values representative of the full range of fuels studied here.

The experiments to measure extinction coefficients are described in the next section. Use of this data in the analysis described in the following section enables accurate determination of soot volume fractions. Finally, the use of the soot volume fractions to make infrared flame radiation calculations is discussed.

EXPERIMENT

Multiwavelength laser transmission experiments are performed with the apparatus shown shematically in Fig. 1. A CW Coherent (model CR-MG) argon/krypton laser operating at either $\lambda = 0.4579\ \mu m$, $0.488\ \mu m$, or $0.5145\ \mu m$ with ~250 mW output and a Spectra-Physics (model 125) helium/neon laser emitting at $\lambda = 0.6328\ \mu m$ and ~50 mW are used. The beams from each laser are superimposed with a beam splitter cube and occupy the same physical path through the flame. After traveling through the flame, the two wavelengths are separated with an equilateral prism. Each beam is then passed through a narrow band pass filter at its own wavelength ($0.003\ \mu m$ bandwidth) to eliminate noise and stray light from the other beam. The beams are each focused with an f = 147 mm lens onto two photodiode detectors (Newport Research Co., model 820 power meter). A reference intensity from each laser is also monitored. The output signals from the detectors are sent through a d.c. amplifier and input to a (Digital Equipment Corp.) AR11 16-channel, 10 -bit A/D converter and stored in a PDP-11/34 minicomputer. Data is read from

the detectors when triggered by a clock tick from the variable frequency timer. The digital display of the timer is filmed with an RCA (model CC002) color video camera connected to a Sanyo (model VTC 8200) video tape recorder.

For each fuel 100 instantaneous stored intensity measurements at each wavelength are correlated with the simultaneous laser pathlengths measured separately for each data point. The laser beam pathlength, L, is taken as the width of the continuous luminosity on a videotape frame. It will be shown in the next section that superposition of the two beams enables determination of mean particle sizes without knowing L, therefore reducing the experimental error.

ANALYSIS

Extinction Coefficient

When a monochromatic beam passes through a homogeneous polydisperse aerosol, the transmitted intensity, I, is related to the initial intensity, I_o, by

$$I(\lambda)/ I_o(\lambda) = \exp(-\tau(\lambda) L) \qquad (1)$$

The intensity and pathlength data I, I_o, and L are used to calculate instantaneous extinction coefficients at each wavelength, $\tau(\lambda)$, which are then averaged. Results at each of two wavelengths give two independent values for the extinction coefficient, τ. These two values are used to find the two parameters in the size distribution, N(r), as explained below. Physically, one would not expect τ to be homogeneously distributed along the pathlength. Thus, it is the average extinction coefficient and average soot volume fraction, along a line of sight which is actually obtained here. From the viewpoint of calculating flame radiation, these averages are precisely the information required.

The extinction coefficient is related to the extinction efficiency, $Q(\lambda,m,r)$, of each individual particle of radius r, and to the particle concentration, N(r)dr, by

$$\tau(\lambda, m, r) = \int_0^\infty N(r)\, Q(\lambda, m, r)\, \pi r^2\, dr. \qquad (2)$$

If spherical particles are assumed, then $Q(\lambda, m, r)$ is well known from Mie scattering theory [10, 19, 20]. A randomly oriented aerosol of chain-like particles, which is probably the situation in turbulent buoyant plumes above pool fires, is not expected to give transmission measurements significantly different from a spherical particle aerosol [10, 21].

Size Distribution

No previous *in situ* carbon particulate detailed size distribution measurements in diffusion flames are known. Most studies use a monodisperse particulate [4,7,9,22]. Size measurements in premixed flames [23] and previous studies here [10] suggest a Gamma distribution [24] with the constraint of a specified ratio of standard deviation to mean particle radius, $\sigma/r_m = 1/2$, as a reasonable functional form. In terms of the most probable radius, r_{max}, and the total particle concentration, N_o, the distribution form is

$$N(r)/No = (27r^3/2r_{max}^4) \exp(-3r/r_{max}) \qquad (3)$$

Note this is a general two parameter distribution. For each fuel, the two extinction coefficients independently measured at separate wavelengths provide two equations for the two unknown size distribution parameters, N_o and r_{max}.

The soot volume fraction is

$$f_v \equiv \frac{4}{3}\pi \int_o^\infty N(r) r^3 dr. \qquad (4)$$

Substituting Eq. (3) into Eq. (4) yields

$$f_v = \frac{54\pi}{38}\,\Gamma(7)\,N_o r_{max}^3 \approx 18.62\,N_o r_{max}^3 \qquad (5)$$

The width choosen for the distribution does not strongly affect f_v. For example, choosing $\sigma/r_m = 1/5$ instead of 1/2 cause only ~15% change in f_v [21].

Normalized Extinction Coefficient Ratio

The Mie theory extinction coefficient [10, 19, 20] and the size distribution of Eq. (3) are substituted into Eq. (5) which is then integrated numerically. The result is shown in Fig. 2 in terms of a non-dimensional extinction coefficient,

$$\tau'(\alpha_{max}, \lambda, m) = \tau/N_o r_{max}^2, \qquad (6)$$

for the four wavelengths used in the experiment. The parameter $\alpha = 2\pi r/\lambda$ describes the interaction of radiation at wavelength λ with a particle of radius r. In the small particle absorption limit, $\alpha \ll 1$, τ is independent of the size distribution and the ratio of two different wavelength τ's becomes

$$[\tau_i/\tau_j]_{absorption} = \lambda_j F_a(\lambda_i)/\lambda_i F_a(\lambda_j), \qquad (7)$$

where the optical properties information is all contained in

$$F_a(\lambda) = \frac{n^2 k}{[n^2-(nk)^2+2]^2 + 4n^4k^2} \qquad (8)$$

In the large particle limit, $\alpha >> 1$, $Q \to 2$ and $\tau_i/\tau_j \to 1$. Thus, the normalized extinction coefficient ratio [10],

$$x_{ij} = [\tau_i/\tau_j - 1]/[\tau_1/\tau_j - 1]_{absorption} , \qquad (9)$$

is adopted as being most convenient for extracting size distribution information from experimental extinction coefficients. Figure 3 shows x_{ij} as a function of most probable radius, r_{max}, for the six different possible wavelength combinations used here.

Using the measured τ_i and τ_j's, the experimental χ_{ij} is obtained from Eqs. (1, 7, 8 and 9). The experimental χ_{ij} is used to extract r_{max} from Fig. 3. Note that since the τ's were superimposed, r_{max} is known independent from L, thereby eliminating a large source of possible error ($\sim$10%). τ' is then determined from r_{max} and Fig. 2. N_o is obtained from Eq. (6) and one of the experimental extinction coefficients. Knowing r_{max} and N_o gives f_v from Eq. (5). Note that since L must be known to obtain τ, the error in measurement of L does affect the accuracy of N_o and f_v.

RESULTS

Experimental Summary

Table 2 presents the measured extinction coefficients and extinction coefficient ratios at several wavelengths for the ten fuels examined. The sample diameter or length in the beam direction, L_o, and laser beam height above each fuel surface, H_b, is also given. The GM designation refers to the well described [25] Products Research Committee cellular plastics material bank. More than one wavelength pair was run when it was necessary to isolate the correct r_{max} in the double valued region of the χ_{ij} vs. r_{max} curves. The experimental standard deviations are shown, calculated from $\gtrsim$100 data points for each fuel. Table 2 thus gives the useful raw data needed in the multiwavelength technique.

Table 3 applies the data in Table 2 and shows the resulting calculatons of χ_{ij}, the most probable radius, the total particle concentration and the soot volume fraction obtained from each wavelength pair run for every fuel. Table 3 demonstrates the consistency of the results among different wavelength pairs run for each fuel. No common pathlength experimental value lies above the theoretical limit for χ_{ij}. This is in contrast to the Ref. 10 results based on the soot optical properties of Dalzell and Sarofim [13] (see Table 3 of Ref. 18). The I/I_o and L data from separate single wavelength experiments previously reported [10] are reinterpreted using Table 1 and are included in Table 3 for comparison with the new common pathlength multiwavelength data for polystyrene foam, polypropylene, acetone and alcohol. The discrepency between the seperate pathlength and common pathlength experiments for polypropylene is due to the low laser light attenuation in this relatively clean flame. The new simultaneous wavelength pair results, which contain less error from pathlength uncertainty, agree very well for different wavelength combinations. The separate pathlength polystyrene foam results are quite compatible with the new common path values, but only the more accurate simultaneous multiwavelength data are included in averages reported for these fuels in Table 4. Note the consistency of the f_v values among different, common path wavelength pairs for all fuels.

Of the fuels which reside in the double valued region of Fig. 3 (i.e., $\chi_{ij} \gtrsim 1$), all except acetone and alcohol lie in the single valued region for at least one alternate wavelength pair. The correct r_{max} for the double

valued case is chosen as closest to the single valued result. For acetone and alcohol, the correct r_{max} is resolved as previously described [10], i.e., by choosing that r_{max} of the double value which is most common among the results from different wavelength pairs.

Discussion

The averages over the wavelength pair results for each fuel in Table 3 are summarized in Table 4. The primary output of this study are the soot volume fractions in the fourth column for the fuels in the first column. The most probable radius and total particle concentration obtained from the multiwavelength technique are listed in the second and third columns, respectively. This table replaces previously reported results [10]. The volume fraction ranking within each fuel type remains unchanged and is consistent with observations of flame luminosity and smokiness. The newly tested wood sample has an f_v and r_{max} very close to that of polypropylene. A detailed uncertainty analysis shows that the experimental error in f_v is $\pm$ ~10% [24, 21].

In the final column of Table 4 are estimates of the fraction of fuel carbon converted to soot (see Ref. 21 for calculation details). A large fraction of the carbon in polystyrene, ~15%, is converted to soot. The respective values for polyurethane and isooctane are ~3% and the remaining fuels result in $\lesssim$ O(1%) fuel carbon conversion to solid particulate. There is reasonable agreement with de Ris [1] who estimated carbon to soot conversion of 18% for polystyrene, 1.9% for PMMA and 5.5% for polypropylene, with a high uncertainty in the latter value. Good quantitative agreement is obtained with

the infrared transmittance and radiance results reported by Buckius and Tien [12] when the more accurate Lee and Tien [18] optical properties are used. Agreement is also achieved with Markstein's soot volume fractions [11] if the larger size of his flames is taken into account. This scaling effect is addressed in a seperate experiment performed here and the results are reported elsewhere [26].

Figure 4 shows detailed size distributions given by Eq. (3), using the experimentally measured parameters in Table 4 for the ten fuels considered. Note that the semi-log plot broadens the actually rather narrow distributions. No fuel was observed to have average particle sizes within the Rayleigh absorption limit for visible radiation. The most probable particle radii are generally twice as large as those calculated in Ref. 10 due to using the revised optical properties in Table 1 instead of the usually [8-12] assumed refractive index from Ref. 13. Only the anamolous foam polystyrene r_{max} has not been substantially altered. The foam samples interestingly have the largest r_{max}, with the two polyurethanes not found to be significantly different.

Infrared Extinction Coefficient

The ability to predict flame radiation from the soot volume fraction results is of primary interest here. In most flames of practical scale soot

emission dominates gas species emission [27]. The nongray soot emissivity can often be represented [28] within 10% by the simple gray expression,

$$\varepsilon = 1 - \exp(-\kappa L) \tag{10}$$

where L is the pathlength or mean beam length and κ is the absorption coefficient or soot emission parameter, defined as

$$\kappa = \tau(\overline{\lambda}) = 36\pi F_{a\sim}(\overline{\lambda}) f_v/\overline{\lambda} \tag{11}$$

where

$$\overline{\lambda} T_{f\ell} = c_2/3.6 = 0.40 \text{ cm K} \quad . \tag{12}$$

$T_{f\ell}$ is an equivalent homogeneous flame temperature and $c_2 = h_{co}/K = 1.44$ cm-°K is Planck's second constant. The derivation of Eq. (10) is based on an empirical fit to the Rayleigh limit nongray emissivity [27,28] which assumes that the spectral extinction coefficient varies as $1/\lambda$ [1,27,29]. This is valid as long as $\alpha << 1$ in the infrared spectral region where most of the flame emission occurs. The Mie theory spectral extinction coefficient based on Eq. (2), the experimental size distributions, and f_v for each fuel, is compared in Fig. 5 to the small particle limit extinction coefficient approximation of Eq. (11). Only the foam mattress result is shown for the two polyurethanes since they are so similar. For fuels with $r_m \lesssim 40$ nm, the approximation is reasonable from $\lambda = 2$ μm to $\lambda = 3$ μm, where the flame emission spectra peak. The approximation underpredicts the Mie theory τ by ~20% for

polystyrene foam, by ~15% for polyurethane foam , and by $\lesssim$0(10%) for the remaining fuels. However, the effect of this error on the flame emissivity may be small. For polystyrene foam with a pathlength of 30 cm and a soot emission temperature of 1200 K, Eqs. (10 and 11) give a soot absorption-emission coefficient of κ = 0.05 cm^{-1} and a soot emissivity of ϵ = 0.78. If actually κ = 0.06 cm^{-1} (20% higher) then ϵ = 0.83, i.e., a 20% underestimate of κ causes only ~6% underestimate of ϵ. Because emissivity determines flame emission, it is significant that propagation of soot emission coefficient error into ϵ is small. It is also important to note that the Mie theory τ is dependent on the size distribution. If the actual size distribution differed, and was narrower than the assumed form in Eq. (3), then the Mie theory τ would be closer to the approximate $\tilde{\tau}$. The volume fraction results are not strongly dependent on the assumed form of the size distribution and use of the approximate expression for $\tilde{\tau}$, which depends on f_v and not on the size distribution, may be even more accurate than it seems from Fig. 5. Within the assumptions and experimental uncertainties, it is reasonable for typical engineering applications to consider all the fuels examined here to generate soot particles which are within the small particle absorption limit for infrared flame radiation calculations and thus permit use of Eqs. (10 and 11).

CONCLUSIONS

Table 4 presents carbon particulate volume fractions of $0(10^{-6})$ and approximate size distributions measured "in situ" for 10 common solid, cellular, and liquid fueled, small scale buoyant diffusion flames. A multiwavelength laser transmission technique [10] has been refined so that beams of two wavelengths from seperate lasers now occupy the same physical path through the flames, thereby reducing experimental errors.

The analysis uses the soot optical properties obtained by Lee and Tien [18] (see Table 1). They were determined from a rigorous consideration of electron band structure and the dispersion constants, in conjunction with independent transmission measurements at visible [10] and infrared [12] wavelengths, and are thus considered to be representative of actual flame soot. These soot refractive indeces are shown here to yield theoretical extinction coefficient ratios as large as experimental values and give consistent results for different wavelength pairs for each fuel. This is in contrast to previous results [10] based on the usually assumed [3, 8, 12] soot refractive indices measured by Dalzell and Sarofim [13] in collected and compressed soot samples.

Polystyrene flames have the largest soot volume fraction ($f_v \sim 3.5 \times 10^{-6}$) and the largest estimate of fuel carbon converted to soot (~15%). The cellular foam fuels, polystyrene and two polyurethanes, are observed to have the largest size particles of all the fuels studied ($r_{max} = 6.2 \times 10^{-2}$ μm and 5.2×10^{-2} μm, respectively). The ranked order of the f_v values is consistent with observed flame luminosity and is in agreement with literature data [11, 12], including results obtained here previously [10]. However, due to use of the new optical properties of Table 1, the values for most probable particulate radii have increased at least twofold and the soot volume fractions have decreased significantly from the original results [10] for all the fuels except the foam polystyrene.

Finally, the mean particle sizes obtained for all fuels indicate that the small particle absorption limit assumption may cause only slight

underestimates ($\lesssim$20% for polystyrene, $\lesssim$15% for polyurethane, and $\lesssim$O(10%) for the remaining fuels) of infrared flame absorption-emission coefficients, but is a reasonable approximaton for flame radiation calculations.

ACKNOWLEDGEMENT

This work was supported by the Center for Fire Research of the U.S.D.O.C. National Bureau of Standards under Grant No. NB 80 NAG-E6839 which was administered by the U.S. Department of Energy under Contract W-7405-ENG-48.

NOMENCLATURE

c_o	speed of propagation of electromagnetic radiation in vacuum
c_2	Planck's second radiation constant, 1.4388 cm °K
f_v	particulate carbon volume/flame volume
$F(\lambda)$	optical properties function
H_b	height above fuel surface
I	radiant intensity
K	Boltzmann constant
L_o	mean beam length or length
m	complex index of refraction
n	real index of refraction
nk	imaginary index of refraction
N	particle concentration
Q	extinction efficiency
r	particle radius
s	experimental standard deviation
T	temperature

Greek

α	$2\pi r/\lambda$
ϵ	emissivity
K	soot emission parameter
λ	wavelength
τ	extinction coefficient
χ_{ij}	normalized extinction coefficient ratio, Eq. (9)

Subscript

a	absorption
b	beam
fl	flame
i	first wavelength
j	second wavelength
m	mean
max	most probable

References

1. de Ris, J., "Fire Radiation - A Review," Seventeenth Symposium (International) on Combustion., The Combustion Institute, 1979, pp. 1003-1016.

2. Erickson, W.D., Williams, G.C., and Hottel, H.C., "Light Scattering Measurements on Soot in a Benzene-Air Flame," Combustion and Flame, Vol. 8, 1964, p. 127.

3. Dalzell, W.H., Williams, G.C., and Hottel, H.C., Combustion and Flame, Vol. 14, 1970, p. 161.

4. Kunugi, M. and Jinno, J., "Determination of Size and Concentration of Particles in Diffusion Flames by a Light Scattering Technique," Eleventh Symposium (International) on Combustion, The Combustion Institute, 1967, pp. 257.

5. Mori, Y. and Makino, K., Bulletin of JSME, Vol. 12, 1951, p. 1448.

6. D'Alessio, A., Di Lorenzo, A., Sarofim, A.F., Beretta, F., Masi, S., and Venitozzi, C., Vol. 5, 1972, p. 263.

7. D'Alessio, A., Di Lorenzo, A., Sarofim, A.F., Beretta, F., Masi, S., and Venitozzi, C., "Soot Formation in Methane-Oxygen Flames," Fifteenth Symposium (International) on Combustion, The Combustion Institute, 1974, p. 1427.

8. Muller-Dethlefs, K., "Optical Studies of Soot Formation and the Addition of Organic Peroxides to Flames," Ph.D. Dissertation, Dept. of Chemical Engineering and Chemical Technology, Imperial College, London, 1979.

9. Kent, J.H., and Wagner, H.Gg., "Soot Formation in a Laminar Diffusion Flame," presented at the Eighteenth Symposium (International) on Combustion, Ontario, Canada, August 1980.

10. Pagni, P.J., and Bard, S., "Particulate Volume Fractions in Diffusion Flames," Seventeenth Symposium (International) on Combustion, The Combustion Institute, 1970, pp. 1017-1028.

11. Markstein, G.H., "Radiative Properties of Plastic Fires," Seventeenth Symposium (International) on Combustion, The Combustion Institute, 1979, p. 1053.

12. Buckius, R.O. and Tien, C.L., Int. J. Heat Mass Transfer, Vol. 20, 1977, p. 93.

13. Dalzell, W.H., and Sarofim, A.F., J. Heat Transfer, Vol. 91, 1969, p. 100.

14. Medalia, A.I. and Richards, L.W., J. Colloid Interface Sci., Vol. 40, 1972, p. 233.

15. Graham, S.C., Comb. Sci. and Tech., Vol. 9, 1974, p. 159.

16. Chippet, S., and Gray, W.A., Comb. and Flame, Vol. 31, 1978, p. 149.

17. Bard, S. and Pagni, P.J., "Comparison of Laser Induced Fluorescence and Scattering in Pool Fire Diffusion Flames," J. Quant. Spec. Rad. Trans., in press, 1980.

18. Lee, S.C. and Tien, C.L., "Optical Constants of Soot in Hydrocarbon Flames," presented at the Eighteenth Symposium (International) on Combustion, Ontario, Canada, August 1980.

19. Mie, G., Ann. Physik, Series 4, 25, 377, 1908.

20. Kerker, M., The Scattering of Light and Other Electromagnetic Radiation, Academic Press, 1969.

21. Bard, S., "Diffusion Flame Particulate Volume Fractions," Ph.D. Dissertation, Dept. of Mechanical Engineering, University of California, Berkeley, 1980.

22. Haynes, B.S., Jander, H., and Wagner, H. Gg., "Optical Studies of Soot-Formation Processes in Premixed Flames", presented at the Eighteenth Symposium (International) on Combustion, Ontario, Canada, August 1980.

23. Wersborg, B.L., Howard, J.B., and Williams, G.L., Fourteenth Symposium (International) on Combustion, The Combustion Institute, 1973, p. 929.

24. Hahn, G.H., and Shapiro, S.S., Statistical Models in Engineering, John Wiley and Sons, Inc. 1968.

25. Tewarson, A., and Pon, R.F., "A Laboratory-Scale Test Method for the Measurement of Flammability Parameters." FMRC Serial No. 22524 Report, Factory Mutual Research Corp., Norwood, Ma., Oct. 1977.

26. Bard, S., and Pagni, P.J., "Spatial Variation of Soot Volume Fractions in Pool Fire Diffusion Flames," Combustion and Flame, in press, 1980.

27. Felske, J.D., and Tien, C.L., Comb. Sci. and Tech., Vol. 7, 1973, p. 25.

28. Yuen, W.W., and Tien, C.L., Sixteenth Symposium (International) on Combustion, The Combustion Institute, 1974, p. 1481.

29. Hottel, H.C., and Sarofim, A.F., Radiative Transfer, McGraw-Hill Book Co., 1967.

Table 1 Soot optical properties, $m(\lambda) = n(\lambda)\,[1 - ik(\lambda)]$

Wavelength, (μm)	$n(\lambda)$	$nk(\lambda)$	$F_a(\lambda)$
0.4579	1.94	0.58	0.033
0.4880	1.94	0.54	0.031
0.5145	1.93	0.52	0.030
0.6328	1.89	0.48	0.029
1.6	1.9	0.80	0.045
2.5	2.1	1.1	0.048
3.0	2.3	1.3	0.046
4.0	2.5	1.5	0.040
5.0	2.7	1.6	0.035

a - Lee, D. and Tien, C.L.: to be published in the Eighteenth Symposium (International) on Combustion, 1980.

Table 2. Measured extinction coefficients, τ_i, and extinction coefficient ratios, τ_i/τ_j, with their experimental standard deviations, s.

	Fuel length L_o cm	Beam ht. H_b cm	Wavelength[a] i	τ_i cm^{-1}	Experimental Standard Deviation s_{τ_i} cm^{-1}	Wavelength Pair[a] i- j	τ_i/τ_j	Experimental Standard Deviation s_{τ_i/τ_j}
Solids								
Polystyrene	7.5	2	1	0.60	0.034	1- 3	1.15[b]	0.08[b]
$(C_8H_8)_n$				0.52	0.028	1- 4	1.50[b]	0.12[b]
				0.40	0.044	3- 4	1.30[b]	0.16[b]
Wood, ASTM Class B Fire Brand, (CH_2O)	15.0	4	1	0.044	0.012	1- 4	2.00	0.26
			4	0.023	0.007			
Polypropylene	7.5	2	1	0.036	0.010	2- 4	1.71	0.29
$(C_3H_6)_n$			2	0.0355	0.009	3- 4	1.53	0.30
			3	0.032	0.008	1- 2	1.01[b]	0.42[b]
			4	0.021	0.005	1- 3	1.13[b]	0.43[b]
						1- 4	1.71[b]	0.63[b]
						2- 3	1.11[b]	0.40[b]
Polymethylmethacrylate	7.5	2	1	0.040	0.007	1- 3	1.18[b]	0.33[b]
$(C_5H_8O_2)_n$, PMMA			3	0.034	0.010	1- 4	1.54[b]	0.23[b]
			4	0.026	0.004	3- 4	1.29[b]	0.32[b]
Foams								
Polystyrene, GM-48	15.0	2	1	0.594	0.060	1- 3	1.03[b]	0.11[b]
$(C_8H_8)_n$			3	0.576	0.027	1- 4	1.28	0.10
			4	0.464	0.040	3- 4	1.24[b]	0.10[b]
Polyurethane, Mattress	15.0	2	1	0.097	0.009	1- 3	1.12	0.13
$(C_{3.2}H_{5.3}ON_{0.23})_n$			3	0.087	0.008	1- 4	1.43	0.11
			4	0.068	0.004	3- 4	1.28	0.11
Polyurethane, GM-21	15.0	2	2	0.083	0.020	2- 4	1.36	0.19
$(C_{3.4}H_{6.1}ON_{0.16})_n$			4	0.061	0.015			
Liquids								
Iso Octane	15.0	4	1	0.083	0.004	1- 3	1.15[b]	0.06[b]
(C_8H_{18})			3	0.072	0.003	1- 4	1.51[b]	0.09[b]
			4	0.055	0.004	3- 4	1.31[b]	0.08[b]
Acetone	15.0	4	2	0.017	0.004	2- 4	1.54	0.32
(C_3H_6O)			3	0.016	0.004	3- 4	1.46	0.16
			4	0.011	0.003	2- 3	1.05	0.36
Alcohol	15.0	4	2	0.010	0.002	2- 4	1.73	0.30
(C_2H_6O)			3	0.009	0.002	3- 4	1.50	0.18
			4	0.006	0.001	2- 3	1.15	0.34

a = i refers to λ_i (λ_1 = 0.4579 μm, λ_2 = 0.4880 μm, λ_3 = 0.5145 μm, λ_4 = 0.6328 μm).

b = computed with separate paths for each wavelength.

Table 3 Experimental flame soot volume fractions and size distributions from multiwavelength experiments.

	Wavelength Pair[a] i-j	χ_{ij}	$r_{max} \times 10^2$ μm	$N_o \times 10^{-9}$ cm^{-3}	$f_v \times 10^6$
Solids					
Polystyrene	1-3	0.647[b]	4.4	2.1	3.3
	1-4	0.864[b]	4.7	1.7	3.3
	3-4	1.08[b]	5.0	1.4	3.3
Wood	1-4	1.72	2.3	1.3	0.29
Polypropylene	2-4	1.82	2.4	1.0	0.27
	3-4	1.88	2.5	0.90	0.26
	1-4	1.23[b]	3.7	0.21	0.20
Polymethylmethacrylate	1-3	0.758[b]	4.0	0.18	0.22
	1-4	0.928[b]	4.5	0.13	0.22
	3-4	1.09[b]	5.0	0.09	0.23
Foams					
Polystyrene, GM-48	1-3	0.231[b]	6.6	0.75	4.0
	1-4	0.486	6.2	0.85	3.8
	3-4	0.851[b]	5.7	1.1	3.8
Polyurethane	1-3	0.494[b]	5.0	0.24	0.55
	1-4	0.735[b]	5.2	0.21	0.56
	3-4	0.991[b]	5.3	0.20	0.56
Polyurethane, GM-21	2-4	0.938	5.2	0.19	0.51
Liquids					
Iso Octane	1-3	0.656[b]	4.4	0.29	0.46
	1-4	0.877[b]	4.7	0.24	0.46
	3-4	1.10[b]	4.9	0.21	0.46
Acetone	2-4	1.40	3.9	0.09	0.10
	3-4	1.62	3.5	0.14	0.11
Alcohol	2-4	1.87	2.4	0.30	0.077
	3-4	1.77	3.0	0.13	0.065

a- i refers to same λ_i as Table 2.

b- computed with seperate paths for each wavelength.

TABLE 4 Summary of soot volume fractions and size distributions

Fuel	$r_{max} \times 10^2$ μm	$N_o \times 10^{-9}$ cm^{-3}	$f_v \times 10^6$	% Carbon converted to soot
Solids				
Polystyrene	4.7	1.7	3.3	15.
Wood	2.3	1.3	0.29	1.4
Polypropylene	2.5	0.93	0.27	0.7
Polymethylmethacrylate	4.5	0.13	0.22	1.2
Foams				
Polystyrene, GM-48	6.2	0.85	3.8	15.
Polyurethane	5.2	0.21	0.56	3.1
Polyurethane, GM-21	5.2	0.19	0.51	3.1
Liquids				
Iso Octane	4.7	0.24	0.46	3.1
Acetone	3.7	0.12	0.11	0.7
Alcohol	2.7	0.19	0.071	0.5

Figure Captions

1. Schematic of apparatus for simultaneous multiwavelength laser transmission measurements.
   $L_{\lambda_i}, L_{\lambda_j}$ -Laser at λ_i or λ_j
   M - Mirror
   B - Beamsplitter
   P - Prism
   T - Digital timer
   C - Video camera
   FL - Focusing lens (f=147 mm)
   F - Bandpass filter (30 A) bandwidth
   $DT_{\lambda_i}, DT_{\lambda_j}$ - Detector for transmitted intensity
   $DR_{\lambda_i}, DR_{\lambda_j}$ - Detector for reference intensity
   OS - Output signal to amplifier and computer

2. Nondimensional extinction coefficient, $\tau' = \tau / N_o r_{max}^2$, versus the most probable particle radius, parameterized in wavelength, with the soot optical properties listed in Table 1.

3. Normalized extinction coefficient ratio, $\chi_{ij} = [\tau_i/\tau_j - 1]/[\tau_i/\tau_j - 1]_{abs}$, versus the most probable particle radius with $\lambda_1 = 0.4579\ \mu m$, $\lambda_2 = 0.4880\ \mu m$, $\lambda_3 = 0.5145\ \mu m$, and $\lambda_4 = 0.6328\ \mu m$, using the soot optical properties of Ref [18] listed in Table 1.

4. Approximate particulate size distribution, N(r), versus particle radius for several fuels.

5. Mie theory and Rayleigh small particle limit extinction coefficient as a function of wavelength with the particulate size distributions and soot volume fractions in Table 4.

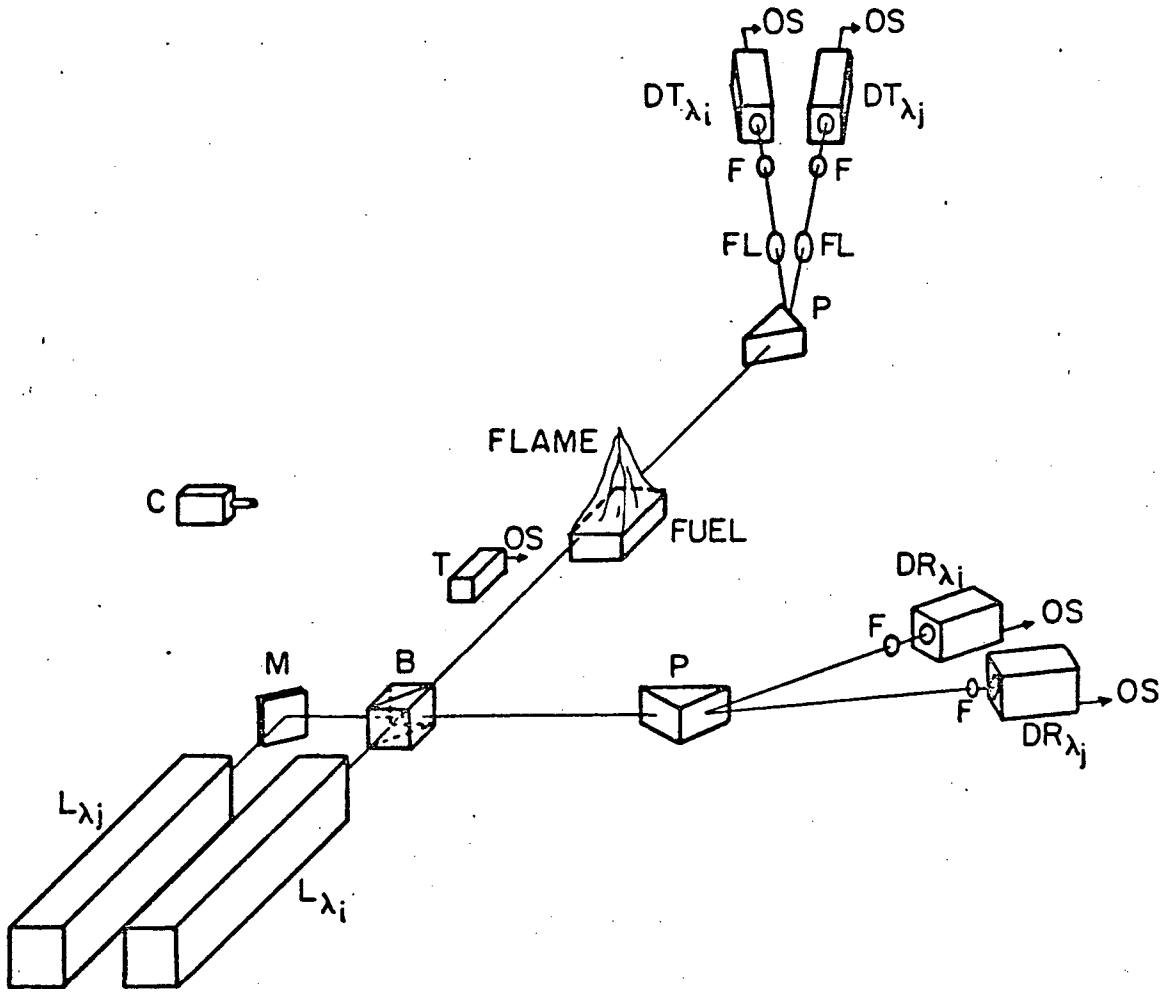

XBL805-5144

Figure 1

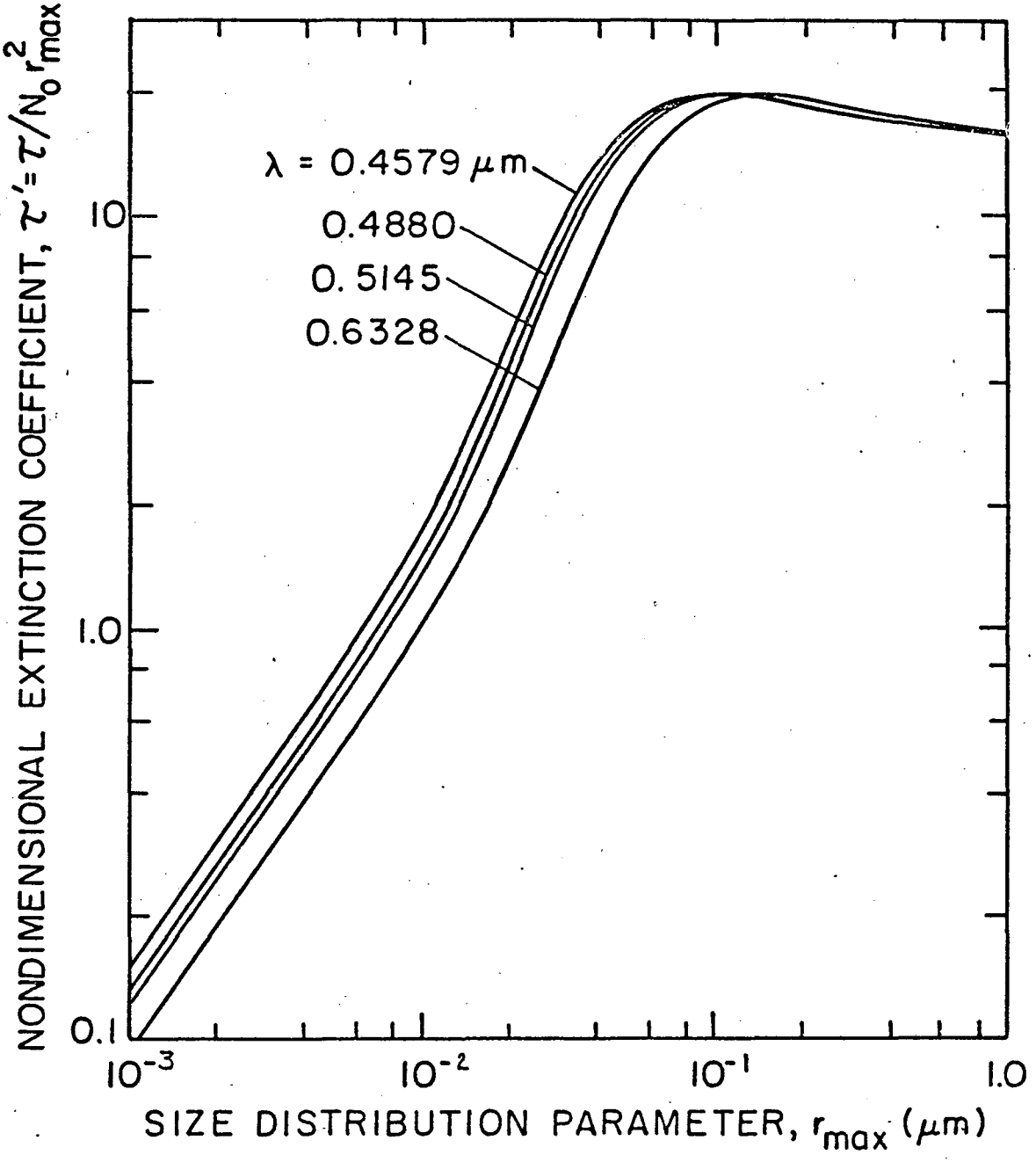

Figure 2

XBL 805-5143

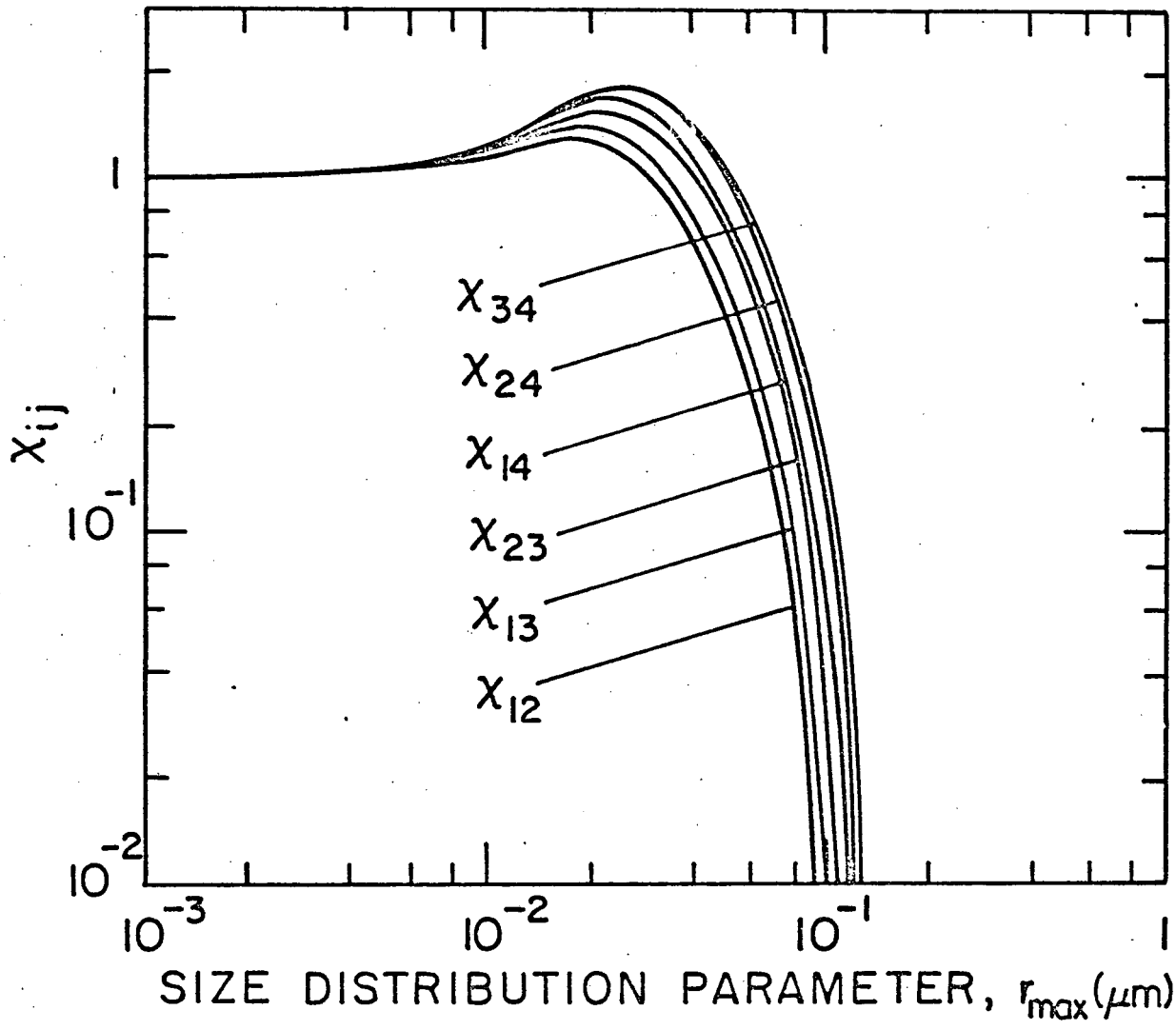

Figure 3

XBL 805-5140

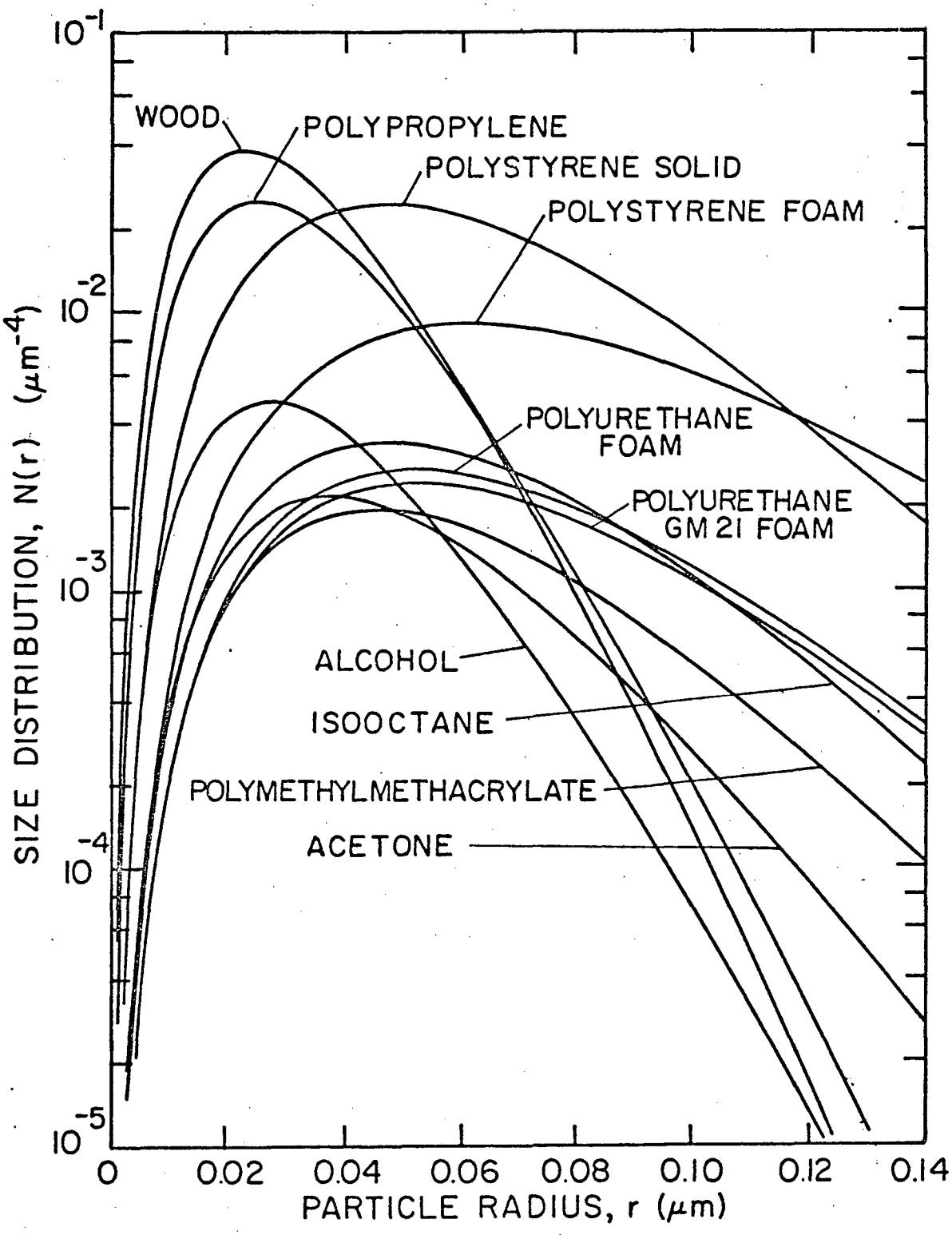
WOOD
POLYPROPYLENE
POLYSTYRENE SOLID
POLYSTYRENE FOAM
POLYURETHANE FOAM
POLYURETHANE GM 21 FOAM
ALCOHOL
ISOOCTANE
POLYMETHYLMETHACRYLATE
ACETONE
SIZE DISTRIBUTION, N(r) (μm⁻⁴)
10⁻¹
10⁻²
10⁻³
10⁻⁴
10⁻⁵
0
0.02
0.04
0.06
0.08
0.10
0.12
0.14
PARTICLE RADIUS, r (μm)
XBL805-5142

Figure 4

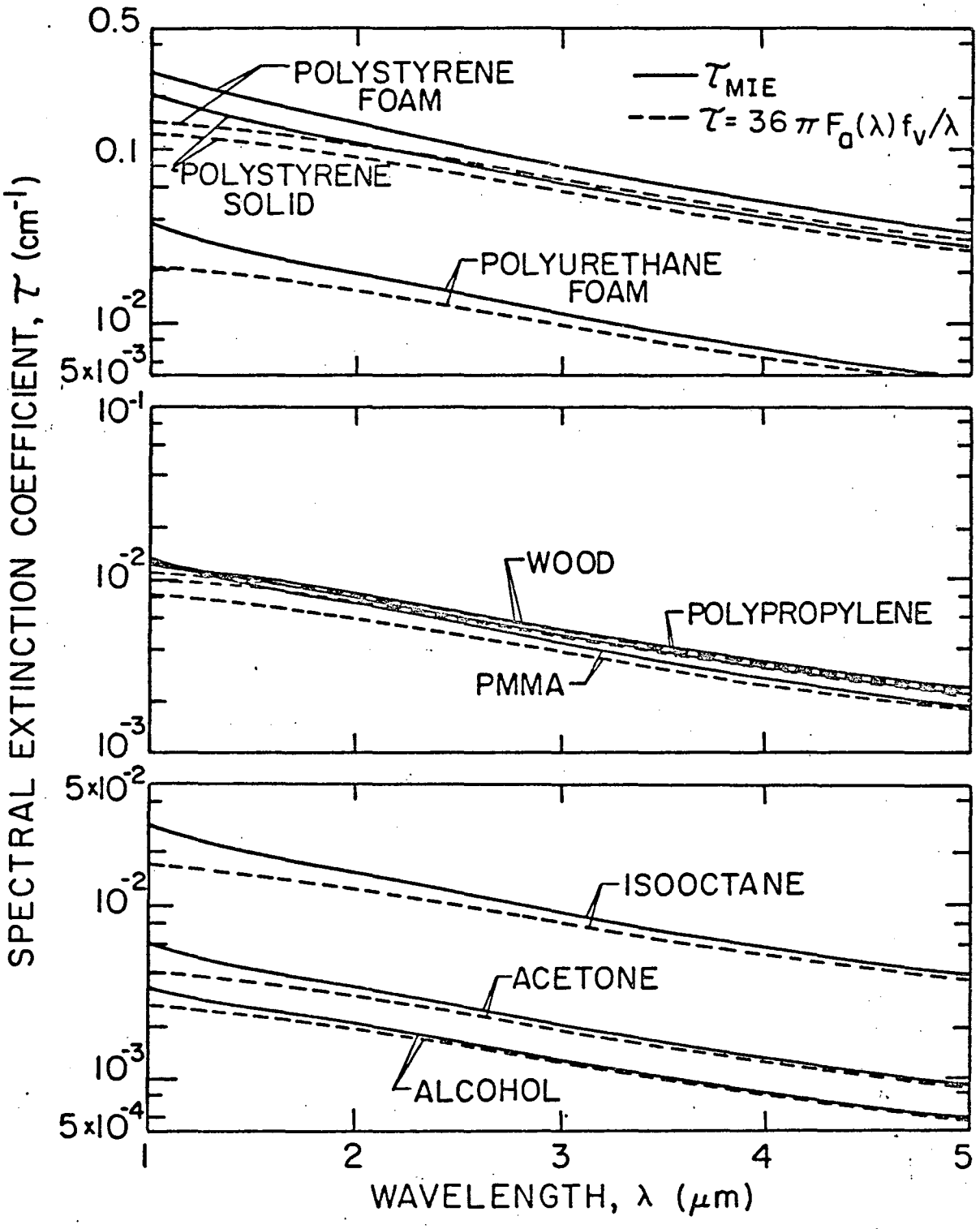

Figure 5

XBL805-5145

TECHNICAL INFORMATION DEPARTMENT
LAWRENCE BERKELEY LABORATORY
UNIVERSITY OF CALIFORNIA
BERKELEY, CALIFORNIA 94720